



HAL
open science

Statistical investigation of the most influent parameters on the cold start of Proton Exchange Membrane Fuel Cell

Mattéo Gantzer, Stefan Giurgea, Daniel Hissel, Nadia Yousfi Steiner

► **To cite this version:**

Mattéo Gantzer, Stefan Giurgea, Daniel Hissel, Nadia Yousfi Steiner. Statistical investigation of the most influent parameters on the cold start of Proton Exchange Membrane Fuel Cell. Vehicle Power and Propulsion Conference, Oct 2024, Washington DC, United States. hal-04953027

HAL Id: hal-04953027

<https://hal.science/hal-04953027v1>

Submitted on 17 Feb 2025

HAL is a multi-disciplinary open access archive for the deposit and dissemination of scientific research documents, whether they are published or not. The documents may come from teaching and research institutions in France or abroad, or from public or private research centers.

L'archive ouverte pluridisciplinaire **HAL**, est destinée au dépôt et à la diffusion de documents scientifiques de niveau recherche, publiés ou non, émanant des établissements d'enseignement et de recherche français ou étrangers, des laboratoires publics ou privés.

Statistical investigation of the most influent parameters on the cold start of Proton Exchange Membrane Fuel Cell

Mattéo Gantzer

*Université de Franche-Comté
Institut FEMTO-ST, FCLAB
UTBM, CNRS
Belfort, France
matteo.gantzer@univ-fcomte.fr*

Stefan Giurgea

*Université de Technologie de Belfort-Montbéliard
Institut FEMTO-ST, FCLAB
UTBM, CNRS
Belfort, France
stefan.giurgea@utbm.fr*

Daniel Hissel

*Université de Franche-Comté
Institut FEMTO-ST, FCLAB
UTBM, CNRS
Institut Universitaire de France (IUF)
Belfort, France
daniel.hissel@univ-fcomte.fr*

Nadia Yousfi-Steiner

*Université de Franche-Comté
Institut FEMTO-ST, FCLAB
UTBM, CNRS
Belfort, France
nadia.steiner@univ-fcomte.fr*

Abstract—Cold start of Proton Exchange Membrane Fuel Cells (PEMFC) remains a challenge for widespread commercialization, especially in embedded application such as in the automotive industry. Here, we propose to statistically study various control and design parameters of a fuel cell system in order to identify the most prevailing ones on the cold start of a PEMFC. A physical model is used to simulate the cold start and the parameters are told apart by calculating their multiple correlation coefficient. It was found that the current density was the most determining factor, along with membrane thickness and initial water content of the ionomer. These results are useful for cold start strategy development and Response Surface Methodology and give perspective on the impact of stack ageing and degradation on cold start performance.

Index Terms—PEMFC, cold start, multiple correlation coefficient

I. INTRODUCTION

In a context of decarbonization of the transportation sector, electric vehicles powered by a hydrogen fuel cell system have seen a growing interest in the past few years, as it avoids local emission of greenhouse gases. Among the various fuel cell technologies, proton-exchange membrane fuel cells (PEMFC) are seen as the most adapted technology thanks to their low-temperature operation (60°C - 85°C) and high power density [1], which are both favorable to embedded applications. Compared to electric vehicles powered solely by batteries, fuel cell vehicles (FCVs) can provide extended driving range and quicker charging time. During winter, FCVs have the advantage of not suffering of shorter driving range due to cold weather and can effectively use the heat from the fuel cell to heat the passenger cabin. However, the ability of

the fuel cell to start under subzero temperatures remains one of the barriers to its widespread use in embedded applications.

During the cold start of a PEMFC, the water generated by the electrochemical reaction freezes and is susceptible to migrate from the catalytic layer (CL) to other layers of the membrane-electrode assembly (MEA) depending on the level of subcooling [2]. Frozen water hinders gas transport and reduces the electrochemically active surface (ECSA) of the CL [3], which causes the cell to shut down and results in structural degradation of the MEA [4], [5]. Fundamental understanding of the freezing mechanism of the water inside the FC and performance optimization have led to many experimental studies to investigate the dependency between various parameters and output performance. Thompson et al. studied the operation of a 50cm² single-cell under isothermal galvanostatic conditions by comparing theoretical and experimental water accumulation in the FC [6]. They reported that higher current density led to lower water accumulation because the void space in the CL was not homogeneously utilized, and that lower current density yielded higher total heat generation. Such conclusions are shared among many following experimental studies. For a non-galvanostatic load control, Hou et al. suggested that progressively increasing the current density would be favorable to the single-cell cold start performance [7]. Water storage in the ionomer allows the FC to operate without ice formation in the MEA. Therefore, a lower hydration of the membrane prior to the startup delays the shutdown of the single-cell FC during isothermal cold start [6], [8]. However, complete drying of the ionomer may cause structural degradation of the membrane and reduces performance in early stages of the startup because of the high ionic resistivity. Pinton et al. showed that there

exists an optimal initial resistivity of the membrane to obtain a maximal current density under potentiostatic load control, which maximizes heat generation inside the MEA [9]. Tajiri commented that a thicker membrane will offer an increased water storage capacity [8]. Similarly, Thompson et al. observed that CL with higher ionomer content allowed longer operation for the isothermal cold start of a single-cell FC [6], since water also accumulates in the hydrophilic ionomer of the CL and thus provides water storage. Hiramitsu et al. observed that CL partially covered with ice performed better with a higher ionomer content. They suggested that the thicker ionomer layer on the agglomerates allowed oxygen to reach additional reaction sites through permeation [10]. Considering non-isothermal cold start of FC stack, the thermal mass of the stack plays an important role in the heating rate of the cells. Oszipok et al. tested a complete FC system with a 6-cell stack and concluded that stacks with high thermal mass would require external heating as the subcooling increases beyond 10°C in order to start successfully operate the stack [11]. Schießwohl et al. tested a FC system with a stack comprising 60 cells and suggested to reduce the thermal mass of the stack by removing coolant circulation [12].

Fuel cells are multi-physics objects and their performance relies on many parameters from mixed domain. Studying the influence of a large number of parameters on an objective function such as the output voltage of a FC would require to perform many experiments or simulations, which is time-consuming and expensive. Thus, dedicated statistical methods have been originally developed in the agricultural industry to require the minimum amount of test to allow many factors to be studied over a range of variations, alleviating the experimental effort [13], [14]. Such methods are called design of experiments and have been applied to the design and control optimization of PEM fuel cells among many other research sectors. In this context, the ANalysis Of VAriance (ANOVA) studies the variability of a response to determine which factors are statistically significant. This allows to study the optimal design of a fuel cell, and is also useful for screening out the most important parameters and to apply the Response Surface Method or to model the response as a mathematical function of a number of factors [15]. Turkmen et al. have used the ANOVA to investigate the optimal design of the anode flow field of a Direct Methanol Fuel Cell (DMFC) composed of parallel channels, with the pressure drop along the channels as the objective function. The parameters were the width of the channels and the distance between channels, and they added the ratio of channel area to the total active area as an additional parameter related to the two others [16]. Al-Hadeeti et al. used the ANOVA to generate a mathematical correlation of the performance of a PEMFC from experiments at various temperatures, flow rates and flow patterns. They obtained a surface response clearly showing the interactions between parameters and determined the optimal performance of the FC [17]

Technical targets of vehicular PEM fuel cells systems are set by the US Department of Energy (DoE), which states that

the ultimate objective for a FCV is to start from -30°C without assistance in 30 seconds and from -40°C with less than 5 MJ of assistance in 30 seconds [18]. From the perspective of a vehicle constructor, such objectives can remain vague or inadequate, since different markets and applications are susceptible to face varying temperatures and cold start frequency during winter, as well as adaptable technical specifications. Unfolding what factors are the most relevant to cold start operation may allow for more adapted and cost-efficient system designs of FCVs, thus supporting industrial-scale commercialization. This paper proposes a methodology to statistically determine the most critical parameters to the cold start of a PEMFC. A 1D physical model is used to simulate the cold start of a fuel cell under various controls and designs. Statistical analysis is then applied to determine the multiple correlation coefficients R^2 , indicating what parameters have the most influence on the performance of the fuel cell.

II. METHODOLOGY

A. Simulation platform

Simulations of the fuel cell stack operation are performed via a 2D + 1D physical model developed in the Matlab/Simulink environment, based on the Bond Graph theory and presented in details in [19], [20]. It consists of connected elementary blocs of two kinds: “R-block” accounting for transport phenomena, and “C-block” performing mass and energy balance (see Fig.1). Equations in the blocks vary depending on the component of the fuel cell, which are the structure, composed of the end plates, collector plates and bipolar plates (BP); gas channel; the gas diffusion electrode (GDE) comprising the gas diffusion layer (GDL), the microporous layer (MPL) and the catalytic layer (CL); and the proton exchange membrane. In-plane transport phenomena are modeled in 2D whereas trough-plane is in 1D. However, due to the parallel design of the gas channels and the fact that no in-plane species transport is considered in the MEA and in the membrane, in-plane modelling is reduced to 1D along the length of the gas channels. The model accounts for convection and diffusion of a two-phase flow in the channels and the GDE, water transport and species permeation through

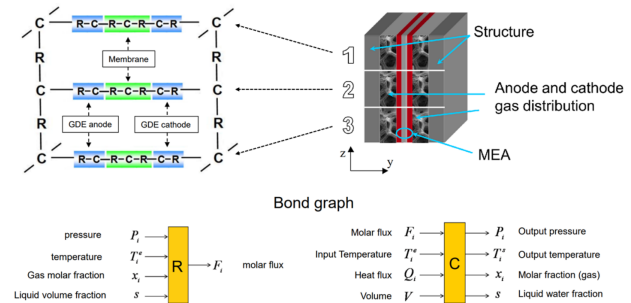


Fig. 1. Bond graph of an elementary cell in the model. It should be noted that the four C-blocks at the ends represent inputs/outputs of the manifolds, and is not bonded to other elementary blocks, since the stack is simplified to n-equivalent cells.

the membrane, and water is considered in liquid, vapor and solid phase in the GDE and the channels. The cell potential is calculated via a modified form of the Butler-Volmer expression based on parameters fitted on polarization curves. Assumptions are that materials in the MEA are isotropic and the model simulates only one cell, which means that the fluidics and the electrochemical response are the same for the n -equivalent cells of the fuel cell stack. However, thermal balance is performed for all the cells so that the model takes into account the mutual heating between them. It can incorporate auxiliaries to model a complete fuel cell system and has thus been used for system design, evaluation and optimization, regulation strategies testing [21], and to study interactions between the system and the fuel cell, regarding heterogeneities [20] and degradation mechanisms inside the cell [22], [23]. This model has been developed for many years and repeatedly validated against experimental data produced during various projects with diverse aims and operational conditions.

B. Statistical study

Statistical study is used to determine the most influential parameters on the cold start of a PEMFC. Sets of design and control parameters \mathbf{x} are generated and used as inputs to the model in order to measure the response of the fuel cell to an objective function y . To obtain a set of responses \mathbf{Y} , it is necessary to generate multiple sets of parameters \mathbf{x} that can be put in the form of a matrix \mathbf{X} . This matrix can be obtained through factorial experimental design, which gives all the combinations of the parameters. However, when dealing with a large number of parameters, it is more reasonable to use an orthogonal array (OA) in order to create a subset of factorial experimental design, thus reducing the number of simulations to be performed. Using an OA combines the advantage of reducing the computational effort and providing sufficient data to extract the most significant parameters [13]. More specifically, to determine the effect of n parameters on an objective function, it is required to have $s > n$, with s the number of lines in the OA, which is the number of simulations or experiments.

The value of the multiple correlation coefficient R^2 associated to a parametrical subset \mathbf{x}_s indicates the share of the variance that can be associated to the variation of \mathbf{x}_s and is calculated:

$$R^2(\mathbf{x}_s) = \frac{q \sum_i (y_i - \bar{y})^2}{\sum_i \sum_j (y_{ij} - \bar{y})^2} \quad (1)$$

y_{ij} is the response associated to a set of input parameters \mathbf{x} , $i = 1, \dots, m$, $j = 1, \dots, q$, where q is the number of levels that the parametrical subset \mathbf{x}_s can take and m is the number of sets for which \mathbf{x}_s is at the level i . y_i is therefore the conditional mean of the subset \mathbf{x}_i , which is the matrix composed of all the vectors \mathbf{x} where \mathbf{x}_s is at the level j , and \bar{y} is the overall mean response of the set of responses \mathbf{Y} . The value of $R^2(\mathbf{x}_s)$ lies between 0 and 1, and the parameters with the highest values of R^2 have the highest influence on the response.

III. RESULTS AND DISCUSSION

The goal is to simulate the startup of a PEM fuel cell for vehicular application under freezing conditions and to determine the most prevalent parameters in its performance. Because it is in equilibrium with environment temperature, the cold start of a FC generally requires a dedicated control strategy to raise the temperature of the cells past the melting point of water. Cold start strategies are classified as assisted, i.e. using an external source of energy to increase the temperature, or self-sufficient. The latter has the advantage of keeping the FC system compact and not relying on an external energy storage device such as a battery, whose state of charge cannot be controlled [24]. However, they are still limited in their ability to effectively start a FC stack for subcoolings of more than 20°C. Various parameters that could significantly influence the performance of the cold start are varied according to an orthogonal array to study their contribution in the variance in the system response. In this study, a self-sufficient cold start strategy is adopted, and chosen control parameters are relatively conventional, so that they are likely to be part of already existing regulation strategies on any embedded FC system. Anodic and cathodic pressure P_a and P_c , stoichiometry St_a and St_c , and relative humidity RH_a and RH_c are considered for inlet flow. The applied electrical load is in galvanostatic mode (i.e. constant current for the duration of the cold start) and the current density J is being varied throughout the simulation runs, as well as the flow in the cooling circuit Q_c and the initial membrane water content λ_{ini} . It is worth noting that since the membrane, electrodes and gas channels are assumed to be in thermodynamic equilibrium when the cell is shut down, the membrane water content is representative of the humidity inside the cell. Ice formation in the porous media is susceptible to modify porous structures of the layers in the MEA [25], so the thickness δ , porosity ϵ , tortuosity τ and mean pore radius R_p of the catalytic layer are considered. The presence of a micro-porous layer (MPL) between CL and GDL at both the anode and the cathode can play a positive role in cold start operation [26]. Therefore, a MPL was considered in this study at the anode and the cathode and their thickness δ and porosity ϵ are added to this study. Ice formation in the porous catalytic layer is quantified with respect to the ice volumetric saturation s , which is the fraction of void space in the porous media that has been filled with ice. Ice saturation impacts gas diffusion properties and reduced the ECSA according to (2) and (3). The exponent γ is a structural parameter which depends on the shape of the ice, and s_{max} the effective ice saturation at which the ECSA is considered to be fully covered by ice and the fuel cell shuts down. These parameters are not properly design parameters of the FC, since they are used to model performance degradation of the stack. However, they are likely to be strongly dependent on the design of the MEA, namely the tortuosity in the case of β and the composition and structure of the CL for γ and s_{max} .

$$D_i^{eff} = D_i(1 - s)^\beta \quad (2)$$

$$a_{eff} = a \left(\frac{s_{max} - s}{s_{max}} \right)^\gamma \quad (3)$$

Since the water storage capacity of the FC is expected to be of paramount relevance, the ionomer volumetric fraction in the CL ϵ_{CL} , the membrane thickness and concentration in hydrophilic sulfonated side chains C_{SO_3} are taken into account. MEA exposed to repeated freeze/thaw cycles can suffer delamination of their layers due to the accumulation of water at interfaces [4]. This causes an increase in mass and charge transport resistance, so a coefficient k is applied to the contact resistance between the CL and the MPL. For reaction kinetics, the electric conductivity of the catalytic layer σ and the Pt loading $WPt\%$ are added to the study.

Two distinct groups of parameters can be distinguished, namely control-based and design-based, and the statistical study of their influence is conducted separately. Table I presents the values taken by the parameters, which comprises their min and max value corresponding to level 1 and 2 respectively in table II. The reference value is the value taken by the parameters of one group when the other one is being tested. The sets are composed of 9 and 16 parameters respectively, so the design of the orthogonal array will be L16 for both [13], with the design-based OA comprising 6 additional columns. The resulting OAs are shown in Table II.

TABLE I
MINIMUM AND MAXIMUM VALUE OF PARAMETERS

Parameter	Min	Max	Reference
Control-based			
P_a (Pa)	1.28E+05	1.73E+05	1.5E+05
P_c (Pa)	1.28E+05	1.73E+05	1.5E+05
St_a	1.7	2.3	1.5
st_c	1.7	2.3	1.5
RH_a (%)	42.5	57.5	40
RH_c (%)	42.5	57.5	0
I (mA/cm ²)	510	690	600
Q_c (m ³ /s/cell)	0.00085	0.00115	1.5E-03
λ_{ini}	5.95	8.05	7
Design-based			
ϵ_{CL}	0.425	0.575	0.5
τ	1	5.5	1
δ_{CL} (m)	8.5E-06	11.5E-06	10E-06
ϵ_{CL}	0.17	0.23	0.2
WPt (mg/cm ²)	0.0034	0.0046	0.004
R_p (m)	8.5E-09	11.5E-09	10E-09
σ_{CL} (S/cm)	17	23	20
s_{max}	0.3	1	1
δ_{MB} (m)	43.35E-06	58.65E-06	51E-06
C_{SO_3} (mol/m ³)	1785	2415	2036.4
δ_{MPL} (m)	0.0000255	0.0000345	30E-06
ϵ_{MPL}	0.425	0.575	0.5
γ^{sol}	1	5.5	1
β	1.5	3	1
k	4.51E-07	6.10E-07	5.30E-07

TABLE II
ORTHOGONAL ARRAYS FOR BOTH SET OF PARAMETERS

Run	P_a ϵ_{CL}	P_c τ	St_a ep	St_c ϵ_{CL}	RH_a $WPt\%$	RH_c R_p	I σ_{CL}	Q_c s_{max}	λ_{ini} δ_{MB}	C_{SO_3}	δ_{MPL}	ϵ_{MPL}	γ^{sol}	β	k
1	1	1	1	1	1	1	1	1	1	1	1	1	1	1	1
2	1	1	1	1	1	1	1	2	2	2	2	2	2	2	2
3	1	1	1	2	2	2	2	1	1	1	1	2	2	2	2
4	1	1	1	2	2	2	2	2	2	2	2	2	1	1	1
5	1	2	2	1	1	2	2	1	1	2	2	1	1	2	2
6	1	2	2	1	1	2	2	2	2	1	1	2	2	1	1
7	1	2	2	2	2	1	1	1	1	2	2	2	2	1	1
8	1	2	2	2	2	1	1	2	2	1	1	1	1	2	2
9	2	1	2	1	2	1	2	1	2	1	2	1	2	1	2
10	2	1	2	1	2	1	2	2	1	2	1	2	1	2	1
11	2	1	2	2	1	2	1	1	2	1	2	2	2	1	2
12	2	1	2	2	1	2	1	2	1	2	1	1	2	1	2
13	2	2	1	1	2	2	1	1	2	2	1	1	2	2	1
14	2	2	1	1	2	2	1	2	1	1	2	2	1	1	2
15	2	2	1	2	1	1	2	1	2	2	1	2	1	1	2
16	2	2	1	2	1	1	2	2	2	1	2	1	2	2	1

Cold start can be seen as a race against the clock between two competing phenomena: the net generation of heat warming up the MEA, stemming from the balance between the heat from the reaction and the losses to the environment and the cooling circuit, and the ice formation in the electrodes gradually covering the ECSA and clogging the pores, due to the necessary production of water by the electrochemical reaction. The heat loss to the environment depends on the materials properties, the environmental temperature and the flow of coolant. The latter is included in this study, whereas other factors are kept constant in the simulations. The thermal power generated by the reaction arises from the chemical potential not being converted to electrical energy. From an electrical standpoint, the chemical potential is described by the thermoneutral potential E_{TN} , so the heat generated is a function of the difference between the thermo-neutral potential and the stack potential V_{stack} :

$$dQ = (E_{TN} - V_{stack})J.S dt \quad (4)$$

where S is the active surface of the MEA in m² and Q is the thermal energy in J.

The ice formation results from a mass and energy balance inside the electrode. As explained in [5], water is first absorbed by the membrane until it reaches saturation, which corresponds to a water content $\lambda = 14$, and no ice is formed in the electrode during this period. The vapor partial pressure in the electrode then increases until vapor saturating pressure is reached and water further generated is assumed to desublimates instantaneously in the CL, as justified further.

The US DoE stipulates that the criterion for a successful cold start is the ability of the stack to deliver 50% of its nominal power in less than 30 seconds [18]. However, one could argue that the success of a cold start ultimately comes down to the ability of the cells to heat up past the melting point of water, preventing further ice formation and melting the ice inside the CL. Accordingly, the most apposite objective function to describe the performance of a fuel cell in freezing conditions is the temperature of the ionomer T_{MB} , which comprises the membrane and the CL. Besides, two additional objective functions are included to grant a better understanding of the

role of each parameter on the two competing phenomena. First, the ice volumetric fraction, which can be expressed as the water generated by the reaction from the time τ_{sat} when the membrane and the electrode become fully saturated:

$$s_c = \int_{t=\tau_{sat}}^{t=30s} n(H_2O) \frac{M(H_2O)}{\rho_{ice}} \quad (5)$$

where $n(H_2O)$ is the production of water, $M(H_2O)$ is the molar weight of water and ρ_{ice} the density of ice.

Second, the gross heat generation inside the cell, which is the integral form of (4) over the whole cold start. The simulations were conducted for a 4-kW stack composed of 15 cells with an active surface of 350 cm², which is close to the characteristics of the stack that will be used for future experiments. Despite the lower rated power compared to typical stacks used for transportation applications, the number of cells and the active surface realistically reflect the thermal behavior of the stack, which is prevalent for cold start simulation. The cooling fluid is Glysantin G20®, which is a 50/50 water and glycol mix, and the environmental temperature was set to -30°C . At such subcooling, the nucleation rate of water is very fast and no water in the supercooled state is found, justifying the assumption of instantaneous desublimation [2]. Finally, the fuel cell operation was simulated for 30 seconds in order to comply with DoE standards.

A. Control-based parameters coefficients

As described in section II-B, the value R^2 of a parameter indicates its influence on an objective function, highlighting the most relevant ones, and table III shows the R^2 values for the three objective functions. Two parameters are proven significant on the generation of ice inside the electrode, the others accounting for less than 1%. The current density is the most determining parameter with 60% of the variance, and the initial membrane water content second with 39%. The amount of water produced inside the cell is directly proportional to the current density, as shown below where F is the Faraday constant.

$$n(H_2O) = \frac{a \cdot J}{2F} \quad (6)$$

Membrane dryness provides the most significant water storage capacity by absorbing the water from the reaction. It is thus expected that the initial membrane water content plays a significant role in the final ice saturation, since it essentially allows the FC to operate free of ice generation over the hydration of the membrane. Fig. 2 shows the repartition of the multiple correlation coefficients across control-based parameters for gross heat generation. The current density has the most influence on the generation of heat, which is in agreement with the expression of Q in (4), however contributions are relatively spread out between the parameters. Anodic pressure, relative humidity and stoichiometry combine for 54% of the variance, which can be explained by the influence of anodic conditions on water back diffusion from cathode to anode and reaction

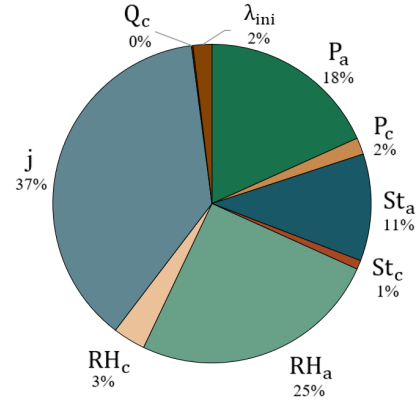


Fig. 2. Control-based parameters R^2 to the gross heat generation Q

kinetics. Ultimately, the overall most influent parameter on the temperature of the membrane after 30 seconds is the current, which is expected since it plays a major role in both competing phenomena.

B. Design-based parameters coefficients

The study of the design-based parameters suggests properties that enhance the performance of a fuel cell under freezing conditions. The dominance of the membrane thickness over all the other parameters regarding ice saturation is in accordance with the previous results, in the way that the ability of the membrane to absorb the produced water and prevent it from freezing is decisive on the final ice volumetric saturation. In that respect, a thicker membrane allows for more water to be stored, since the water content is a measure of the number of water molecule relative to the number of hydrophilic sulfonated groups inside de membrane. However, the concentration of sulfonated groups is also present in the study but appear to have a negligible influence on the saturation. The contributions to gross heat generation are shown in Fig. 3. It should be reminded that, for galvanostatic operation, a lower stack voltage leads to more heat being generated, provided that

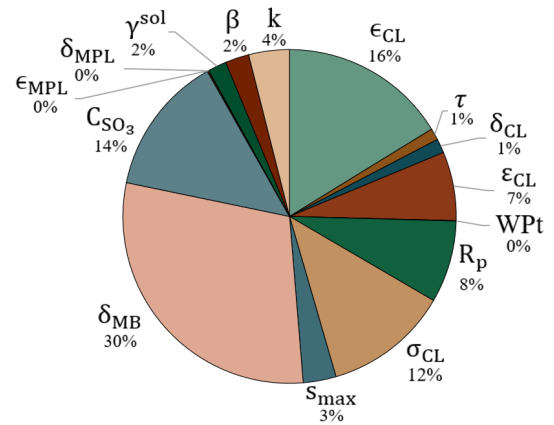


Fig. 3. Design-based parameters R^2 to the gross heat generation Q

the load demand is met. Proton transport across the ionomer depends on the level of hydration of the membrane, and a dry membrane will thus be an important source of resistive losses. Similarly, ionomer content in the CL serves the purpose of channeling the proton to the reaction sites, so the effects of a dry ionomer extends to the CL. This is in accordance with the significance of water transport-related parameters δ_{MB} , ϵ_{CL} and C_{SO_3} of respectively 30%, 7% and 14%. Contact resistance coefficient k , reflecting delamination of the layers, as well as catalytic layer electric conductivity σ_{CL} add up to resistive losses. CL porosity, tortuosity, pore radius and the exponent β have an influence on gas diffusion properties, and, in turn, on the ability of the cell to supply the CL with enough reactants to maintain the rate of the electrochemical reaction. A decay in gas diffusion properties of the cell is susceptible to lead to operation below the stoichiometry ratio of the reaction, leading to a collapse of the voltage. These contributions combine for more than 27% of all contributions to the variance. Membrane water uptake properties are again the most prevailing in the temperature of the cell, and the effects on ice and heat generation are akin. A dry membrane allows for a longer operation free of ice generation while causing notable resistive losses enhancing heat generation, and the variance in the membrane temperature is explained almost completely by the membrane thickness.

IV. CONCLUSION

This paper proposes a methodology based on the multiple correlation coefficient to statistically determine the most

influential parameters on the performance of a PEMFC under freezing conditions. A well-established 1D multiphase model of PEMFC is used to simulate the operation of a 4-kW fuel cell under freezing conditions, two sets of parameters and three objective functions are studied. The main contributions of this article are listed below:

- The study of control-based parameters screens out the most significant factors to investigate for the development of a dedicated cold-start regulation strategy or to use the Response Surface Method and develop a surrogate model.
- Ranking of design-based parameters provides insights to the most impactful design choices for the development of stacks resilient to cold-start operation. Elucidating what parameters determine the performance of the cold start may also give insights on the robustness of a stack or a cold start strategy against ageing and degradation over time
- The generation of heat inside the cell shows a distribution on multiple parameters across both sets, with the most influential parameters being the current density and the thickness of the membrane, accounting for 37% and 30% of the contributions to the variance of control and design parameters respectively.
- Ice saturation relies predominantly on the water generation and the water storage capacity of the membrane. The current density is responsible for 99% of control-based parameters contributions, and membrane thickness and concentration in sulfonated side-chains making up for 44% of design-based parameters.
- Variance in the membrane temperature is explained at 99% by one parameter in each set of parameters, which are current density and membrane thickness respectively.

TABLE III
R² VALUES FOR THE THREE OBJECTIVE FUNCTIONS

Parameter	s_c	Q	T_{MB}
<i>Control-based</i>			
P_a	0.0001	0.1777	0.0002
P_c	0.0000	0.0165	0.0001
St_a	0.0000	0.1057	0.0001
St_c	0.0000	0.0089	0.0004
HR_a	0.0000	0.2464	0.0000
HR_c	0.0001	0.0322	0.0000
I	0.6025	0.3654	0.9965
Q_C	0.0000	0.0014	0.0000
λ_{ini}	0.3967	0.0186	0.0021
<i>Design-based</i>			
ϵ_{CL}	0.0001	0.01623	0.0000
τ	0.0021	0.0114	0.0000
δ_{CL}	0.0000	0.0137	0.0000
ϵ_{CL}	0.0003	0.0667	0.0000
WPt	0.0004	0.0004	0.0011
R_p	0.0000	0.0796	0.0000
σ_{CL}	0.0000	0.1210	0.0000
s_{max}	0.0009	0.0319	0.0024
δ_{MB}	0.9965	0.2956	0.9927
C_{SO_3}	0.0000	0.1353	0.0000
δ_{MPL}	0.0000	0.0012	0.0000
ϵ_{MPL}	0.0000	0.0004	0.0000
γ^{sol}	0.0017	0.0180	0.0036
β	0.0000	0.0231	0.0000
k	0.0087	0.0337	0.0003

ACKNOWLEDGMENT

This work is part of the French research project DURASYS-PAC, and was supported by the EIPHI Graduate School (contract ANR-17-EURE- 0002) 11 and the Region Bourgogne Franche-Comté.

REFERENCES

- [1] F. Gao, B. Blunier, and A. Miraoui, *Modélisation de piles à combustibles à membrane échangeuse de protons: physique, méthodes et exemples* (Génie électrique). Paris: Hermès science publications-Lavoisier, 2011, ISBN: 978-2-7462-3136-8.
- [2] Y. Ishikawa, M. Shiozawa, M. Kondo, and K. Ito, "Theoretical analysis of supercooled states of water generated below the freezing point in a PEFC," *International Journal of Heat and Mass Transfer*, vol. 74, pp. 215–227, Jul. 2014. DOI: 10.1016/j.ijheatmasstransfer.2014.03.038.
- [3] Y. Luo and K. Jiao, "Cold start of proton exchange membrane fuel cell," *Progress in Energy and Combustion Science*, vol. 64, pp. 29–61, Jan. 2018. DOI: 10.1016/j.pecs.2017.10.003.

- [4] Q. Yan, H. Toghiani, Y.-W. Lee, K. Liang, and H. Causey, "Effect of sub-freezing temperatures on a PEM fuel cell performance, startup and fuel cell components," *Journal of Power Sources*, vol. 160, no. 2, pp. 1242–1250, Oct. 2006. DOI: 10.1016/j.jpowsour.2006.02.075.
- [5] X. Yang, J. Sun, X. Meng, S. Sun, and Z. Shao, "Cold start degradation of proton exchange membrane fuel cell: Dynamic and mechanism," *Chemical Engineering Journal*, vol. 455, p. 140823, Jan. 2023. DOI: 10.1016/j.cej.2022.140823.
- [6] E. L. Thompson, J. Jorne, W. Gu, and H. A. Gasteiger, "PEM fuel cell operation at 20°C. i. electrode and membrane water (charge) storage," *Journal of The Electrochemical Society*, vol. 155, no. 6, B625–B634, Aug. 2008. DOI: 10.1149/1.2905857.
- [7] J. Hou, H. Yu, M. Yang, W. Song, Z. Shao, and B. Yi, "Reversible performance loss induced by sequential failed cold start of PEM fuel cells," *International Journal of Hydrogen Energy*, vol. 36, no. 19, pp. 12444–12451, Sep. 2011. DOI: 10.1016/j.ijhydene.2011.06.100.
- [8] K. Tajiri, Y. Tabuchi, F. Kagami, S. Takahashi, K. Yoshizawa, and C.-Y. Wang, "Effects of operating and design parameters on PEFC cold start," *Journal of Power Sources*, vol. 165, no. 1, pp. 279–286, Feb. 2007. DOI: 10.1016/j.jpowsour.2006.12.017.
- [9] E. Pinton, Y. Fourneron, S. Rosini, and L. Antoni, "Experimental and theoretical investigations on a proton exchange membrane fuel cell starting up at subzero temperatures," *Journal of Power Sources*, vol. 186, no. 1, pp. 80–88, Jan. 2009. DOI: 10.1016/j.jpowsour.2008.09.056.
- [10] Y. Hiramitsu, N. Mitsuzawa, K. Okada, and M. Hori, "Effects of ionomer content and oxygen permeation of the catalyst layer on proton exchange membrane fuel cell cold start-up," *Journal of Power Sources*, vol. 195, no. 4, pp. 1038–1045, Feb. 2010. DOI: 10.1016/j.jpowsour.2009.08.016.
- [11] M. Oszcipok, M. Zedda, J. Hesselmann, *et al.*, "Portable proton exchange membrane fuel-cell systems for outdoor applications," *Journal of Power Sources*, vol. 157, no. 2, pp. 666–673, Jul. 2006. DOI: 10.1016/j.jpowsour.2006.01.005.
- [12] E. Schießwohl, T. Von Unwerth, F. Seyfried, and D. Brüggemann, "Experimental investigation of parameters influencing the freeze start ability of a fuel cell system," *Journal of Power Sources*, vol. 193, no. 1, pp. 107–115, Aug. 2009. DOI: 10.1016/j.jpowsour.2008.11.130.
- [13] G. S. Peace, *Taguchi methods: a hands-on approach*. Reading, Mass Wokingham: Addison-Wesley, 1993, 522 pp., ISBN: 978-0-201-56311-5.
- [14] L. Moore, M. McKay, and K. Campbell, "Combined array experiment design," *Reliability Engineering & System Safety*, vol. 91, no. 10, pp. 1281–1289, Oct. 2006. DOI: 10.1016/j.ress.2005.11.024.
- [15] B. Wahdame, D. Candusso, X. Francois, F. Harel, J. Kauffmann, and G. Coquery, "Design of experiment techniques for fuel cell characterisation and development," *International Journal of Hydrogen Energy*, vol. 34, no. 2, pp. 967–980, Jan. 2009. DOI: 10.1016/j.ijhydene.2008.10.066.
- [16] A. C. Turkmen, C. Celik, and H. Esen, "The statistical relationship between flow channel geometry and pressure drop in a direct methanol fuel cell with parallel channels," *International Journal of Hydrogen Energy*, vol. 44, no. 34, pp. 18939–18950, Jul. 2019. DOI: 10.1016/j.ijhydene.2019.04.034.
- [17] F. Al-Hadeethi, M. Al-Nimr, and M. Al-Safadi, "Using the multiple regression analysis with respect to ANOVA and 3d mapping to model the actual performance of PEM (proton exchange membrane) fuel cell at various operating conditions," *Energy*, vol. 90, pp. 475–482, Oct. 2015. DOI: 10.1016/j.energy.2015.07.074.
- [18] U.-S. D. O. Energy, *DOE technical targets for fuel cell systems and stacks for transportation applications*, 2022. [Online]. Available: <https://www.energy.gov/eere/fuelcells/doe-technical-targets-fuel-cell-systems-and-stacks-transportation-applications> (visited on 01/11/2024).
- [19] P. Schott and P. Baurens, "Fuel cell operation characterization using simulation," *Journal of Power Sources*, vol. 156, no. 1, pp. 85–91, May 2006. DOI: 10.1016/j.jpowsour.2005.08.034.
- [20] C. Robin, M. Gerard, J. d'Arbigny, P. Schott, L. Jabbour, and Y. Bultel, "Development and experimental validation of a PEM fuel cell 2d-model to study heterogeneities effects along large-area cell surface," *International Journal of Hydrogen Energy*, vol. 40, no. 32, pp. 10211–10230, Aug. 2015. DOI: 10.1016/j.ijhydene.2015.05.178.
- [21] M. Gerard, J.-P. Poirot-Crouvezier, D. Hissel, and M.-C. Pera, "Oxygen starvation analysis during air feeding faults in PEMFC," *International Journal of Hydrogen Energy*, vol. 35, no. 22, pp. 12295–12307, Nov. 2010. DOI: 10.1016/j.ijhydene.2010.08.028.
- [22] M. Mayur, M. Gerard, P. Schott, and W. Bessler, "Lifetime prediction of a polymer electrolyte membrane fuel cell under automotive load cycling using a physically-based catalyst degradation model," *Energies*, vol. 11, no. 8, p. 2054, Aug. 8, 2018. DOI: 10.3390/en11082054.
- [23] I. Elferjani, G. Serre, B. Ter-Ovanesian, and B. Normand, "A coupling approach between metallic bipolar plates corrosion and membrane chemical degradation in the proton exchange membrane fuel cells," *International Journal of Hydrogen Energy*, vol. 46, no. 63, pp. 32226–32241, Sep. 2021. DOI: 10.1016/j.ijhydene.2021.06.215.
- [24] A. A. Amamou, S. Kelouwani, L. Boulon, and K. Agbossou, "A comprehensive review of solutions and strategies for cold start of automotive proton exchange

membrane fuel cells,” *IEEE Access*, vol. 4, pp. 4989–5002, 2016. DOI: 10.1109/ACCESS.2016.2597058.

- [25] E. Cho, J.-J. Ko, H. Y. Ha, *et al.*, “Characteristics of the PEMFC repetitively brought to temperatures below 0°C,” *Journal of The Electrochemical Society*, vol. 150, no. 12, A1667, 2003. DOI: 10.1149/1.1621877.
- [26] X. Xie, R. Wang, K. Jiao, G. Zhang, J. Zhou, and Q. Du, “Investigation of the effect of micro-porous layer on PEM fuel cell cold start operation,” *Renewable Energy*, vol. 117, pp. 125–134, Mar. 2018. DOI: 10.1016/j.renene.2017.10.039.